A Biomechanically Motivated Two-Phase Strategy for Biped Upright Balance Control

Muhammad Abdallah

Robotics Locomotion Lab
Stanford University, CA 94305
U.S.A.

mesam@stanford.edu

Ambarish Goswami

Honda Research Institute
Mountain View, CA 94041
U.S.A.

agoswami@honda-ri.com

Abstract - **Balance maintenance and upright posture recovery under unexpected environmental forces are key requirements for safe and successful co-existence of humanoid robots in normal human environments. In this paper we present a two-phase control strategy for robust balance maintenance under a force disturbance. The first phase, called the *reflex phase,* is designed to withstand the immediate effect of the force. The second phase is the *recovery phase* where the system is steered back to a statically stable "home" posture. The reflex control law employs angular momentum and is characterized by its counter-intuitive quality of "yielding" to the disturbance. The recovery control employs a general scheme of seeking to maximize the potential energy and is robust to local ground surface feature. Biomechanics literature indicates a similar strategy in play during human balance maintenance.**

Index Terms – Biped robot, disturbance rejection, balance, posture recovery, potential energy.

1. MOTIVATION

Future humanoid robots are expected to freely reside within common human environments and to be physically more interactive with their surroundings. A key factor for their successful co-existence with humans lies in their capacity to withstand unexpected external forces without the loss of balance. A failed postural recovery may result in a fall which can badly damage the machine itself and/or injure people in the vicinity. We wish to develop a control strategy such that biped robots can appropriately respond to unknown force disturbances from the surroundings.

This paper focuses on the specific problem of balance maintenance during upright stance which is to be distinguished from balance maintenance during gait. We take our cue from biomechanics research [10] which points out the very different nature of the two apparently related problems and how human beings employ specific control strategies to deal with them.

We recognize two main phases during a balance maintenance scenario. The first phase is the *reflex phase* in which the body generates a rapid movement to quickly absorb a disturbance force. As the disturbance force subsides, the body attempts to recover its original posture. This is called the *recovery phase*.

In accordance with these two phases of the balance maintenance scenario, we employ a two-phase control strategy. The reflex controller rapidly generates an increase in angular momentum to correctly compensate for the destabilizing effect of the disturbance. In doing so it accepts a posture deviation. The objective of the recovery controller is to compensate for this postural deviation. It is assumed that the final destination of the robot is a statically stable posture.

Biomechanical studies indicate that human beings adopt a similar strategy in response to an unexpected perturbation [11]. As shown in Fig. 1, the immediate effect of a loss of balance in the forward direction is an accelerated rotation of all the available limbs towards the front (clockwise). This has the effect of reversing the direction of the ground friction force from the forward (Fig. 1a) to the backward direction (Fig 1b). This backward friction force causes the center of mass (CoM), denoted by G, to travel backwards and the center of pressure (CoP), denoted by P, to return securely under the foot support, which is precisely what is intended. Once comfortable, the forward rotation stops and the body returns to a statically stable upright posture (Fig. 1c).
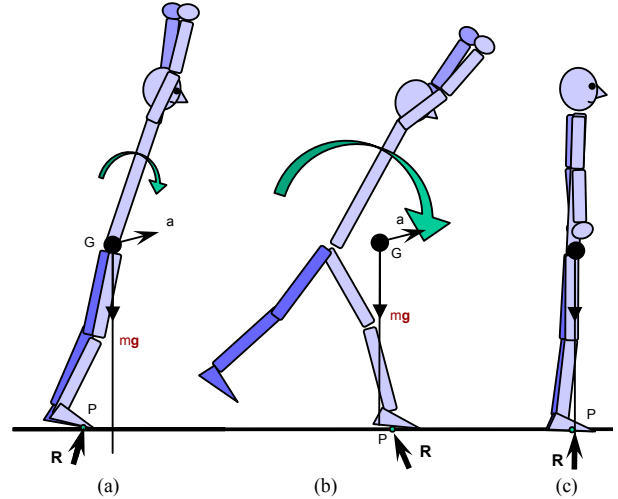

Fig. 1. A typical strategy employed by human beings in response to an unbalanced posture caused by a disturbance [11].

In the above example, Fig. 1b and Fig. 1c represent the reflex and the recovery phases, respectively.

Our dynamic analysis explains the interesting but counter-intuitive forward acceleration of the body during the reflex phase (Section 4). This movement is quantified by the rate-of-change of the angular momentum. In the

recovery phase we seek to guide the system to its maximum potential energy (PE), a strategy that is independent of the local ground slope (Section 5).

Sugihara & Nakamura proposed a similar partitioned strategy for disturbance absorption [18]. We will provide the justification for this partitioning. In addition, we will present fundamental physical measures for the control of each phase.

2. ROBOT MODEL

We created a planar upright robot model as the basis of our analysis and simulation. It is a single-leg plus HAT (head-arms-trunk) model in the sagittal plane, somewhat standard in the postural balance literature. The model contains four limbs: the foot, shank, thigh, and HAT. These rigid body limbs are inter-connected through three actuated joints: the ankle, knee, and hip. The robot model is 175 cm tall, with anthropometric link geometry and mass.

The foot is free to leave the ground; however, we assume that friction is sufficient to prevent slip. The robot has 4 kinematic foot/ground contact states as shown in Fig. 2. In the *Flatfoot phase*, the foot is flat against the ground. In the *Toe phase* and *Heel phase* the foot pivots around the toe or the heel respectively. In the *Airborne phase*, the foot completely lifts off of the ground. The robot has three degrees of freedom (DOF) in the Flatfoot phase, four DOF in each of both the Toe and Heel phases and six DOF in the Airborne phase. We developed a state-transition machine to detect and trigger a switch to a different phase. For this purpose we tracked a number of kinematic and kinetic parameters such as the foot position, foot angle, ground reaction-force (GRF), and the CoP.

The standard formulation for the equation of motion is,

$$\boldsymbol{\tau} = \boldsymbol{M}(\boldsymbol{q})\ddot{\boldsymbol{q}} + \boldsymbol{C}(\boldsymbol{q},\dot{\boldsymbol{q}}) + \boldsymbol{G}(\boldsymbol{q}). \qquad (1)$$

For n degrees of freedom: $\boldsymbol{\tau}$ is the nx1 vector of generalized torques, $\boldsymbol{M}$ is the nxn inertia matrix, $\boldsymbol{C}$ is the nx1 vector of Coriolis and centrifugal terms, $\boldsymbol{G}$ is the nx1 vector of gravity terms, and $\boldsymbol{q}$ is the nx1 vector of configuration variables.
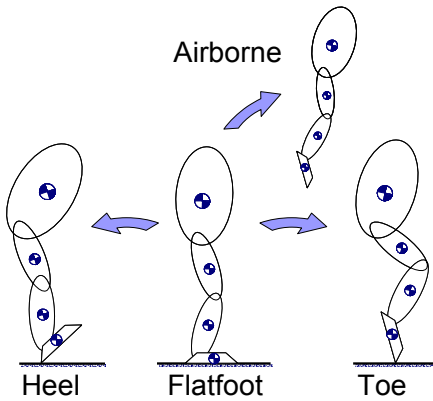

Fig. 2. A planar upright humanoid model for balance studies. The model has 4 foot/ground contact states: Flatfoot, Toe, Heel and Airborne.

Most of our simulation revolves around the Flatfoot model which is the most secured. The motion equation is

fully actuated for the Flatfoot phase with $\boldsymbol{\tau} = (\tau_a\ \tau_k\ \tau_h)^{\mathrm{T}}$ and $\boldsymbol{q} = (q_a\ q_k\ q_h)^{\mathrm{T}}$. The Toe and Heel phases have one degree of under-actuation, and the Airborne phase has 3 degrees of under-actuation.

3. CONTROLLABILITY OF UPRIGHT BALANCE

Robotics literature uses a variety of terminologies to imply the ability of a robot to survive a perturbation to its planned states. Examples include: balance maintenance, postural stability, dynamic stability, gait stability, tip-over stability, and tumble stability. Unlike static stability, no precise and universal definition of dynamic stability exists [1, 3].

The disparate nature of the biped gait and posture control and some existing confusion prompt us to clearly indicate the scope of the current study. From the outset, we wish to point out that *home posture controllability*, and not what is loosely termed as *stability*, is our focus. Below we present a conceptual description of our position.

The phenomena of balance and fall in legged entities arise fundamentally due to the under-actuation and unilateral force constraint at the foot/ground interface [2, 3]. The state of balance of such a system is captured by ground-based points such as the CoP, which is also known as the zero-moment point (ZMP) [2, 3, 9, 12, 13], and the FRI point [3].

The CoP must remain within the convex hull of the ground support area. As long as it is within the interior of the foot, the system has greater flexibility to withstand perturbation since the CoP can move in any direction along the ground. Once the CoP reaches the boundary, it looses a degree of freedom in its motion and the system becomes under-actuated. This is depicted in Fig. 3, where the possible movement directions of the CoP are indicated in both the interior and at the boundary of the foot.

For a robot with a flat foot resting on a level surface, a CoP within the interior of the foot implies that the foot is stationary and flat against the ground. A CoP on the boundary indicates that the foot is either pivoting about its edge or on the verge of pivoting. For our robot model, a CoP within the interior of the foot is represented by the Flatfoot phase, while a CoP on the boundary is represented by the Toe or Heel phase respectively.
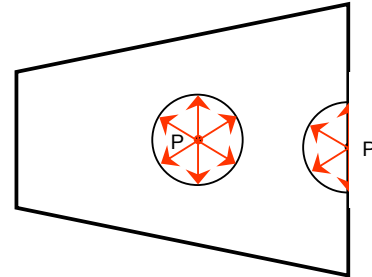

Fig. 3. Robot controllability is related to the CoP location in the foot support area. While located within the support area, the CoP can move in all directions, providing full controllability. At the perimeter, the CoP can move in only certain direction, which results in the loss of a degree of controllability.

Robotics literature often equates location of the CoP/ZMP in the interior of the foot with the stability of the robot [19-22]. This is not an accurate description of the physical phenomenon, mainly because there is no agreed upon definition of stability. For example, a robot can maintain a flat foot and still tumble to the ground with its trunk. On the other hand, the foot can start to turn on its toe and still manage to bring itself back without falling. The key is not stability but the robot's *controllability* at the current state.

The term controllability is usually associated with linear systems where it refers to the ability of a controller to reach a fixed final state from any given initial state [23]. An equivalent description may be provided for our non-linear system where the home posture is the final state and the set of states from which the home posture is reachable is the controllable space. Note however that the concepts of controllability and reachability are completely equivalent for linear systems but not for non-linear systems [23]. Our description is equivalent to what has been recently formulated in terms of viability theory [24].

Our objective in this paper is to maintain the controllability of the robot. We will do so by regulating the CoP to keep it in the interior of the foot, away from the edge, and thus keep the system fully actuated.

4. REFLEX PHASE

A   Disturbance Absorption

Disturbance absorption implies the ability of a robot to withstand a disturbance without losing controllability. Using the stated idea of the CoP regulation, we will be able to identify the underlying physics of disturbance absorption. We will also show that the disturbance absorption ability of a biped is enhanced by divorcing it from posture recovery.

Let us explore the equation for the CoP. The CoP can be computed from the external and inertial forces acting on the system. For a planar ground surface, the position P of the CoP with respect to a general point C on the ground:

$$ \boldsymbol{r_{CP}} = \frac{\boldsymbol{n} \times \left(\boldsymbol{\dot{H}_G} + \boldsymbol{r_{CG}} \times m(\boldsymbol{a_G} - \boldsymbol{g}) - \boldsymbol{r_{CF}} \times \boldsymbol{F} \right)}{\boldsymbol{n} \cdot \boldsymbol{R}} , (2) $$

where $\boldsymbol{r_{CP}}$ is the position vector from C to CoP, $\boldsymbol{n}$ is the ground normal, $\boldsymbol{\dot{H}_G}$ is the centroidal angular momentum, $\boldsymbol{r_{CG}}$ is the vector from C to the CoM, m is the total mass of the robot, $\boldsymbol{a_G}$ is the CoM acceleration, $\boldsymbol{F}$ is the net "non-ground" external forces, $\boldsymbol{r_{CF}}$ is the vector from C to the point of application of $\boldsymbol{F}$, and $\boldsymbol{R}$ is the GRF.

If we apply this equation to our planar robot standing on a horizontal surface and under a horizontal disturbance force $\boldsymbol{F_{dist}}$, we obtain the following equation:

$$ x_P = \frac{mg}{d} x_G + \frac{\dot{H}_C}{d} + \frac{y_F F_{dist}}{d} \quad (3) $$

$$ d = \dot{L}_y + mg. $$

where x_P is the x-coordinate of the CoP, x_G is the x-coordinate of the CoM, $\dot{H}_C$ is the time-derivative of the

angular momentum about point C, and $\dot{L}_y$ is the y-component of the time-derivative of linear momentum. Note that d is a positive quantity. When the robot starts out at the standing position, it is at a singularity for motion in the y direction and so the change in the y direction is relatively small. It is very difficult for the CoM to fall faster than gravity which is required to make d negative.
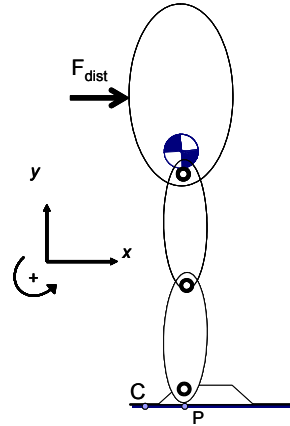
Let us examine (3). For static conditions, the CoP starts out coinciding horizontally with the CoM. A positive F_{dist} tends to move the CoP in the forward or positive direction, see Fig. 4. The larger the force, the closer the CoP gets to the front edge of the foot. This can be countered by a negative $\dot{H}_C$ which occurs when the robot "falls forward" in the clockwise direction. The more the robot can increase its rate of angular momentum, the larger a force it can absorb. Alternatively, if the robot "resists" the force by holding rigid or accelerating backwards, it will push the CoP further ahead and closer to the edge. A human exhibits such behaviour. Given a push in the back, the human accelerates the torso and flails the arms to increase the rate of angular momentum.

Any attempt at posture recovery during the disturbance will oppose the increase in forward angular momentum. It amounts to resisting the force and would push the CoP closer to the edge. This is why the two phases, disturbance absorption and posture recovery, need to be separated.

One problem is that the robot cannot rotate in an accelerated fashion for a long time. As the robot rotates, the CoM moves forward, making it a more and more difficult problem to keep the CoP within the foot. We would thus like to implement the disturbance absorption in such a way as to keep the horizontal position of the CoM constant. We can rewrite (3) by expressing the angular momentum about the CoM rather than C,

$$ x_P = x_G + \frac{\dot{H}_G - y_G \dot{L}_x}{d} + \frac{y_F F_{dist}}{d} \quad (4) $$

$$ d = \dot{L}_y + mg. $$

Fig. 4. The upright robot subjected to a horizontal force disturbance, F_{dist}.

The middle term of this equation represents the "falling forward" term that is used to absorb the disturbance. It now allows us to isolate the component that moves the CoM

horizontally, L_x. Due to the redundancy in our system, we can control the angular and the linear momentum independently. We can now use $\dot{H}_G$ to absorb the disturbance while regulating $\dot{L}_x$ to limit the CoM forward motion. The next section contains the models used to control momenta.

B. Momentum Controller

Both L and H_G are vector functions of the configuration variables q and their derivatives. They are linear with respect to the derivatives. In matrix form they are expressed as:

$$H_G = A(q)\dot{q} \tag{5}$$
$$L = D(q)\dot{q}. \tag{6}$$

In general, A and D are 3xn matrices and are functions of q. For our planar robot, A is reduced to a 1xn matrix and D to a 2xn matrix. A and D are matrices that are "inertial" in nature; their derivation is available elsewhere [6].
The formulae for the time-derivatives are:

$$\dot{H}_G = A(q)\ddot{q} + \dot{A}(q,\dot{q})\dot{q} \tag{7}$$
$$\dot{L} = D(q)\ddot{q} + \dot{D}(q,\dot{q})\dot{q}. \tag{8}$$

The first row of (8) contains the x-component of the linear momentum,

$$\dot{L}_x = D_x\ddot{q} + \dot{D}_x\dot{q}. \tag{9}$$

The concept of the Disturbance Absorption controller was to produce an $\dot{H}_G$ to absorb the disturbance while regulating $\dot{L}_x$ to maintain the CoM. To that end, we solved for (7) and (9) simultaneously using the Moore-Penrose pseudo-inverse,

$$\ddot{q} = \begin{bmatrix} A \\ D_x \end{bmatrix}^+ \begin{pmatrix} \dot{H}_G^* - \dot{A}\dot{q} \\ \dot{L}_x^* - \dot{D}_x\dot{q} \end{pmatrix} \tag{10}$$

We then used the following control law for the momentum:

$$\dot{H}_G^* = k_1(x_P - x_G)$$
$$\dot{L}_x^* = -k_2 L_x \tag{11}$$

where k_i is a positive gain. The desired torques were then computed using (1) for the flatfoot phase.
Note, the controller in (10) is attempting to control the joint accelerations on a second-order system. It is therefore not stable; however, it is adequate for our purpose of displaying the concept. A better control law is needed for a practical implementation. We will present the simulation results in Section 5 of the paper.

C. A Note on Linear and Angular Momenta

There has been recent interest in angular momentum and its possible exploitation for biped balance and gait [4, 6, 8, 17]. Biomechanical investigations conjecture that humans tightly regulate their angular momentum for a large class of movements [17]. Goswami & Kallem proposed $\dot{H}_G$ as an inherent physical measure of the postural stability of a biped [4]. H_G has also been used by others as a tool for generating and controlling humanoid motion [6, 8].
It can be shown, however, that neither H_G nor $\dot{H}_G$ sufficient as a complete descriptor of the controllability of a biped. A redundant system such as a humanoid robot can move about with infinitely many possible motions all of which maintain zero H_G. It can swing about and fall to the ground without creating any angular momentum, and we have encountered this in our simulation.

5. RECOVERY PHASE

A. Maximum Potential Energy

The home posture should be an easily definable, statically stable configuration that is applicable to all bipeds. We suggest the home position to be the configuration of the robot which minimizes the static joint torques. The static torque components are gravity induced. They are minimized when the gravity forces are passively supported by the structure of the robot rather than being actively compensated by the joint motors. Such a posture would greatly reduce the energy expenditure, as we experience from our effortless upright stance compared to one with a bent knee.
Others have explored this idea in anthropomorphic bipeds. Popovic has shown that humans minimize their joint torques during motion [17]. Khatib, et al. use the concept of minimal joint torques due to gravity to resolve the redundancy of a humanoid in relation to a task [7], and show that the resulting postures look natural for a human being. We will expand this idea to a more general concept that better defines the standing posture, and use it to create simple control laws for posture recovery.
The static joint torques are expressed in the G vector of the equation of motion (1). They are thus minimized when the norm of G, $\|G\|$, is minimized. Note that G equals the gradient of the potential energy function V,

$$G = \frac{\partial V}{\partial q}^T. \tag{12}$$

This leads us to a more general concept for the standing posture: the posture that maximizes PE.
This is a simple but powerful concept. Bipeds hold their CoM at the highest location, storing the PE to draw on it in moving in any direction with the least expenditure of energy [15]. So the posture of maximum PE minimizes the static joint torques as well as maximizes the mobility in the horizontal plane.

B. Natural Posture Recovery (NPR)

We now have two concepts for defining the standing posture: Maximum PE, and Minimum G. The two are

closely related with a few differences. Each leads to a simple control law for standing posture recovery.

The first control law maximizes the potential energy by guiding the robot to the peak of the V function. It uses the property that the gradient points in the direction of steepest ascent. The law was determined using (12),

$$\dot{q} = kG. \tag{13}$$

k is a constant positive gain. We will refer to this control law as the *Gradient method*.

The second law finds the minimum G by relating the rate-of-change of G to the rate-of-change of the joint variables q. Since G is a function of q, we can find the following Jacobian relationship:

$$\dot{G} = J(q)\dot{q}$$
$$\dot{q} = J^{-1}\dot{G}. \tag{14}$$

For n degrees of freedom, J is the nxn matrix of first-order partials, $\partial G/\partial q$. G is minimized by relating its time-derivative to the error, $G-G_{min}$. Any non-prismatic manipulator will have a maximum for PE; hence, the minimum $\|G\|$ occurs at $G_{min} = 0$. The control law is thus:

$$\dot{q} = -kJ^{-1}G, \tag{15}$$

where k is a constant positive gain. We refer to this law as the *Hessian method*, for reasons that we will see.

C. Understanding the Two Laws

As mentioned, the two laws are closely related with small differences. For a scalar multi-variable function, a local maximum occurs when it passes the first and second derivative tests:

$$\left(\frac{\partial V}{\partial q}\right)^T = 0 \tag{16}$$

$$q^T\left[\frac{\partial^2 V}{\partial q^2}\right]q < 0. \tag{17}$$

In the first test (16), the gradient of V must equal zero. This occurs for all the *stationary points* of the function: any local extrema or a saddle-point. In the second derivative test (17), the nxn matrix $[\partial^2 V/\partial q^2]$ is known as the Hessian matrix. Evaluated at any stationary point, the left-hand side of (17) indicates the nature of the point. It indicates whether the point is a local maximum (less than zero), local minimum (greater than zero), or a saddle-point (equal to zero).

For any non-prismatic robot, the potential energy function is a continuous sinusoidal function with a global maximum, global minimum, and several saddle-points. It has no local extrema. Fig. 5 shows the potential energy of our robot as a function of the ankle and knee joints.
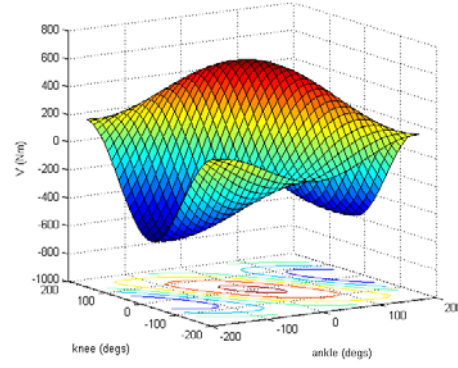

Fig. 5. The potential energy of our robot with a locked hip. Note its "well-behaved" nature.

The J matrix in (14) is thus the Hessian of our potential energy function.

The absence of any local extrema guarantees that the Gradient method will find the maximum potential energy. This occurs for one single posture. At this posture, the static joint torques will also be minimized so that $G = 0$. This minimum G criteria, however, has additional solutions known collectively as the stationary points. There is one maximum and one minimum configuration, as well as several saddle-points. At these points, the potential energy increases with respect to one joint and decreases with respect to another. Fig. 6 shows examples of these stationary configurations for our robot. Note, some of these configurations may be inconsistent with other physical considerations such as joint limits and ground contact.
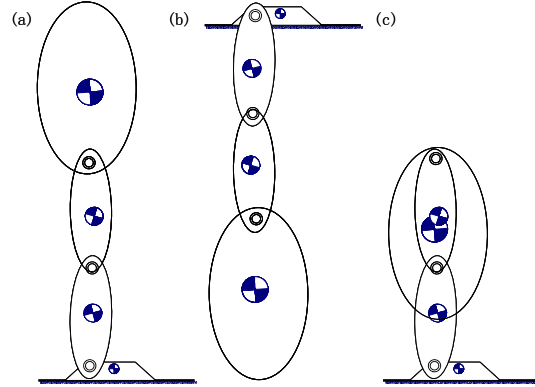

Fig. 6. The "stationary points" where $G=0$: (a) maximum PE, (b) minimum PE, (c) saddle-point.

D. Performance of the NPR Methods

We have tested both methods on our simulation. The robot started out with a crouched pose and the two methods were applied to recover its home position. They were applied in real-time with no precomputed final position. We developed a graphical simulation of the robot in *OpenGL*, a graphics application programming interface, to show the results. Fig. 7 and 8 contain snapshots of the frames.
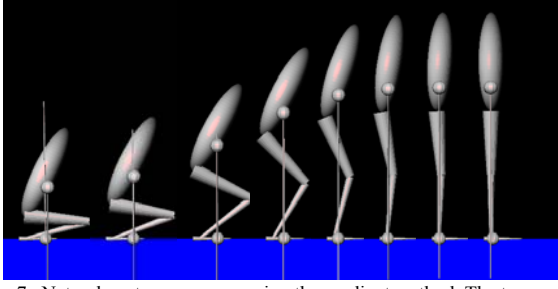
Fig. 7. Natural posture recovery using the gradient method. The top marker represents the CoM and the bottom marker represents the CoP. The frames are taken in intervals of 0.5 seconds.
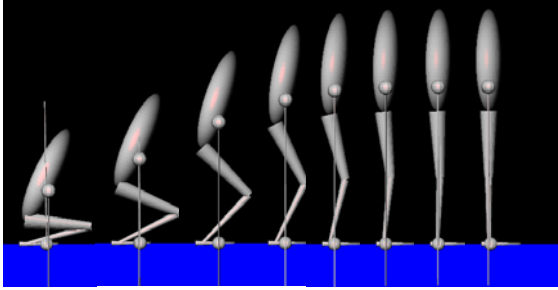

Fig. 8. Natural posture recovery using the Hessian method. The frames are taken in intervals of 0.5 seconds.

For the given initial condition, both methods behaved similarly. The gains determine the second-order behavior of the response for both methods. They were chosen to produce comparable behaviour and response times. Both NPR methods have no consideration for the CoP position. The CoP excursions can be limited by reducing the gains. We thus used a variable gain—one that started small and monotonically increased.

We observed several general differences between the two methods. The Hessian method produced smaller values and fluctuation in both the joint-torques and the CoP position. Unfortunately, the Hessian method has other solutions as we described, and can run into singularities for J. The Gradient method, on the other hand, is much more computationally efficient. It produces behaviours that appear very "natural." It also tends to produce oscillations about the final position that are more significant than the Hessian method.

An additional simulation test for the natural posture recovery scheme consists of positioning the robot on an inclinable plane, such as a swinging table. We incorporated both the variable kinematic constraint and the movement dynamics of the swinging motion into the robot. The task of the controller is to steer the robot to its home position while the table surface oscillates sinusoidally. Fig. 9 displays a series of snapshots where the robot successfully returns to the home position.

We would like to highlight the strengths of the two control laws. They are both able in real-time to guide the robot to the posture that minimizes the static joint torques. They apply a simple strategy that does not need any numerical computation and does not need a pre-planned configuration or trajectory. All they need is to construct the PE function, which is very simple, and to feedback the joint variables.
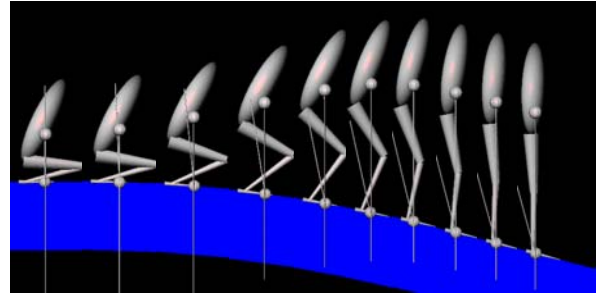

Fig. 9. The ground is rotating while the robot recovers its home posture using the Gradient Method. The frames were shifted vertically to smoothly display the rotation of the ground.

5. SIMULATION RESULTS

The full Reflex-Recovery control strategy was applied to our robot. A horizontal disturbance force F_{dist} was applied to the center of the trunk as shown in Fig. 3. The overall controller applied the disturbance absorption technique during the application of the disturbance force. It then switched to the Hessian method for posture recovery as the force subsided.

Based on a static analysis with locked joints, the maximum F_{dist} our robot can sustain before the foot starts to rotate is 96 N. In contrast, with the presented controller the robot can withstand 300 N, a rather large disturbance force, for a duration of 0.1 seconds. The controller succeeded in absorbing the disturbance and recovering the natural posture. Fig. 10 shows snapshots of the robot recovering. Our current model does not have the knee joint limits; hence we see the backward-bent knee.

6. CONCLUSION AND FUTURE WORK

An effective strategy for maintaining the postural stability of bipeds involves two phases: a reflex phase and a recovery phase. During a disturbance, the biped induces an increasing angular momentum $\dot{H}_G$ to fall along the direction of the disturbance force to maintain controllability. This is a strategy also witnessed in humans.

The biped then initiates a recovery strategy. Maximum potential energy provides a compelling criterion for defining the home posture. It also provides efficient, real-time compatible control laws for posture recovery that are independent of the ground slope.
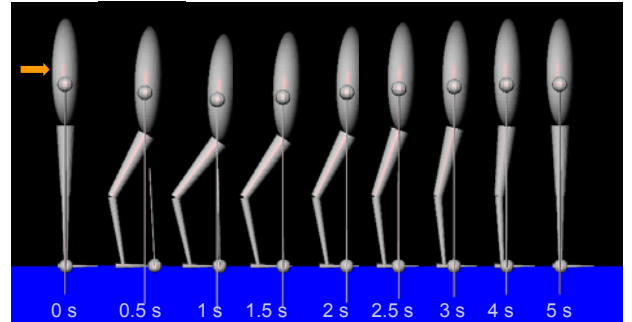

Fig. 10. A disturbance force of 300 N was applied to the robot for 0.1 seconds. The controller absorbed the disturbance during the first 0.1 seconds and then recovered the natural posture.

The stability of the robot depends on controlling the rate-of-change of momentum. A robust controller for $\dot{H}_G$ and $\dot{L}$ is required. We would also like to formulate a unified control strategy for natural posture recovery that combines both methods for the advantages of each. Finally, we would like to extend our model to include a full 3D biped robot that incorporates joint limits and motor saturation torques.

ACKNOWLEDGEMENTS

REFERENCES

[1] D. Katic and M. Vukobratovic, "Survey of Intelligent Control Techniques for Humanoid Robots," *Journal of Intelligent and Robotic Systems*, vol. 37, pp. 117-141, 2003.

[2] M. Vukobratovic, B. Borovac, D. Surla, and D. Stokic, *Biped Locomotion: Dynamics Stability, Control and Application*. Springer-Verlag, New York, 1990.

[3] A. Goswami, "Postural Stability of Biped Robots and the Foot Rotation Indicator (FRI) Point," *International Journal of Robotics Research*, vol. 18, no. 6, pp. 523-533, 1999.

[4] A. Goswami and V. Kallem, "Rate of Change of Angular Momentum and Balance Maintenance of Biped Robots," *IEEE Conference on Robotics and Automation*, 2004, New Orleans, LA.

[5] K. Hirai, M. Hirose, Y. Haikawa, and T. Takenaka, "The Development of the Honda Humanoid Robot," *IEEE Conference on Robotics and Automation*, 1998, Belgium, pp. 1321-1326.

[6] S. Kajita, F. Kanehiro, K. Kaneko, K. Fujiwara, K. Harada, K. Yokoi, and H. Hirukawa, "Resolved Moment Control: Humanoid Motion Planning Based on the Linear and Angular Momentum," in *International Conference on Intelligent Robots and Systems*, 2003, Las Vegas, NV, USA, pp. 1644-1650.

[7] O. Khatib, J. Warren, V. De Sapio, and L. Sentis, "Human-Like Motion from Physiologically-Based Potential Energies," *On Advances in Robotics Kinematics*, Springer 2004.

[8] K. Mitobe, G. Capi, and Y. Nasu, "A New Control Method for Walking Robots Based on Angular Momentum," *Mechatronics*, vol. 14, pp. 163-174, 2004.

[9] Sardain, P. Bessonnet, G. "Forces Acting on a Biped Robot. Center of Pressure—Zero Moment Point." *IEEE Transactions on Systems, Man and Cybernetics*, Part A, vol. 34, No: 5. pp. 630- 637 2004.

[10] Winter, D. "Human balance and posture control during standing and walking". *Gait & Posture*, vol. 3, pp. 193-214, 1995.

[11] Hopper, B. J. "The Mechanics of Human Movement". American Elsevier Publishing Company, Inc., New York, 1973.

[12] Todd, D. J. "An Introduction to Legged Robots." Kogan Page Limited, London, U. K. 1981

[13] H. Hemami. "Reduced Order Models for Biped Locomotion." *IEEE Trans. On Systems, Man and Cybernetics* Vol. 8, pp. 321-325, 1978

[14] Vukobratovic, M. 1973. "How to control artificial anthropomorphic systems", *IEEE Trans. On Systems, Man and Cybernetics v*ol. 3, no. 5pp. 497--507, 1973.

[15] M. Feldenkrais, *Body and Mature Behaviour*. International Universities Press, New York, 1949.

[16] P. Baerlocher and R. Boulic, "Task-Priority Formulations for the Kinematic Control of Highly Redundant Articulated Structures," *IEEE IROS*, 1998, Victoria, Canada, pp. 323-329.

[17] M. Popovic, A. Hofmann, and H. Herr, "Angular Momentum Regulation During Human Walking: Biomechanics and Control," *IEEE Conference on Robotics and Automation*, 2004, pp. 2405-2411.

[18] T. Sugihara, and Y. Nakamura, "Whole-Body Cooperative COG Control through ZMP Manipulation for Humanoid Robot," *IEEE Conference on Intelligent Robots and Systems*, 2002.

[19] M. Vukobratovic, and B. Borovac, "Zero-Moment Point—Thirty Five Years of its Life," *International Journal of Humanoid Robotics*, vol. 1, no. 1, 2004, pp. 157-173.

[20] K. Harada, S. Kajita, K. Kaneko, and H. Hirukawa, "Pushing Manipulation by Humanoids Considering Two Kinds of ZMPs," *IEEE Conference on Robotics and Automation*, 2003, pp. 1627-1632.

[21] Q. Huang, et al, "Balance Control of a Biped Robot Combining Off-line Pattern with Real-Time Modification," *IEEE Conference on Robotics and Automation*, 2000, pp. 3346-3352.

[22] M. Yagi, and V. Lumelsky, "Biped Robot Locomotion in Scenes with Unknown Obstacles," *IEEE Conference on Robotics and Automation*, 1999, pp. 375-380.

[23] M. Vidyasagar, "Nonlinear Systems Analysis." Prentice-Hall, Englewood Cliffs, NJ. 1993.

[24] P.-B. Wieber. 2002. "On the stability of walking systems." *International Workshop on Humanoid and Human Friendly Robotics*